for *Fgfr2*, *Fgfr2*$^{Neo\text{-}S252W}$, *Fgfr2*^{S252W}, *Cre*, and *sFGFR2IIIc*^{S252W}*-3xFLAG*. The primers for *Fgfr2*, *Fgfr2*$^{Neo\text{-}S252W}$, *Fgfr2*^{S252W}, and *sFGFR2IIIc*^{S252W}*-3xFLAG* have been described previously (Holmes et al., 2009; Suzuki et al., 2012) (Fig. 1A, B). The primers for Cre were 5′ -CCTGTTTTGCACGTTCACCG-3′ and 5′ -ATGCTTCTGTCCGTTTGCCG-3′ (290 bp) (Fig. 1B). All experiments were performed in accordance with protocols certified by the Institutional Animal Care and Use Committee of Tokyo Medical and Dental University (#0120272A).

Protein preparation and western blot analysis

Serum was collected from wild-type and *sFGFR2IIIc*^{S252W} mice. FLAG-tagged sFGFR2IIIc^{S252W} protein was purified using a FLAG M Purification Kit (Sigma, St. Louis, MO, USA) according to the manufacturer instructions. Samples were loaded onto a 10% SDS-polyacrylamide gel and transferred to a polyvinylidene difluoride membrane (Amersham Biosciences, Piscataway, NJ, USA). The membrane was incubated with an anti-FLAG antibody (Sigma), and then probed with a horseradish peroxidase-conjugated anti-mouse IgG (Cell Signaling, Danvers, MA, USA). Bound antibodies were detected using an ECL Plus Western Blotting Detection System (Amersham Biosciences) according to the manufacturer's instructions.

μCT imaging protocols of mouse skulls

All mouse samples were scanned at 45 kV, 200 μA, and 12 μm/voxel using a high-resolution X-ray micro-CT system (SMX-100CT; Shimadzu, Kyoto, Japan). BMD, calvaria, and IFS

width were calculated from the raw data by three-dimensional image analysis software (TRI/3-D-BON; Ratoc, Tokyo, Japan). Portions were considered bones with a BMD of more than 120 mg/cm^3. The position of the skull images was calibrated based on the skull base and midline. In coronal section images that showed the narrowest sagittal suture, ROIs were defined as 20 pixels in width and 30 pixels away from the tip of the parietal bone. The IFS width was measured in frontal view with a BMD threshold in 300 mg/cm^3.

Histological analysis

Tissues were fixed in 4% paraformaldehyde/PBS or 10% formalin and embedded in paraffin. Serial transverse sections (10 μm) were stained with hematoxylin and eosin (H&E). To visualize calcium deposits and acid mucosubstances, the IFS was stained with Alizarin red and Alcian blue, respectively.

Statistical analysis

Kruskal-Wallis and Dunn's post hoc tests were used to assess the differences in body weight, BMD, and IFS width. Chi-square and Fisher's exact tests were used to evaluate phenotypic differences. Chi-square tests were used to evaluate differences in the birth prevalence of each genotype from the expected ratio. A p-value of <0.05 was considered statistically significant. Bonferroni corrections were applied for multiple comparisons.

Acknowledgements

We thank Dr. Shigetaka Kitajima (Tokyo Medical and Dental University) for providing *EIIa-Cre* mice and all of the members of our laboratories for assistance. This study was supported by Grants-in-Aid for Scientific Research (Nos. 18209060 and 23390471) and the Global (21st Century) Center of Excellence (COE) Program, International Research Center for Molecular Science in Tooth and Bone Diseases from the Ministry of Education, Culture, Sports, Science, and Technology of Japan.

References

Anderson J, Burns HD, Enriquez-Harris P, Wilkie AO, Heath JK. 1998. Apert syndrome mutations in fibroblast growth factor receptor 2 exhibit increased affinity for FGF ligand. Hum Mol Genet 7:1475-1483.

Chen L, Li D, Li C, Engel A, Deng CX. 2003. A Ser252Trp [corrected] substitution in mouse fibroblast growth factor receptor 2 (Fgfr2) results in craniosynostosis. Bone 33:169-178.

Cohen MM, Jr., Kreiborg S. 1996. Suture formation, premature sutural fusion, and suture default zones in Apert syndrome. Am J Med Genet 62:339-344.

Cohen MM, Jr., Kreiborg S, Lammer EJ, Cordero JF, Mastroiacovo P, Erickson JD, Roeper P, Martinez-Frias ML. 1992. Birth prevalence study of the Apert syndrome. Am J Med Genet 42:655-659.

Coumoul X, Deng CX. 2003. Roles of FGF receptors in mammalian development and congenital diseases. Birth Defects Res C Embryo Today 69:286-304.

Eswarakumar VP, Lax I, Schlessinger J. 2005. Cellular signaling by fibroblast growth factor receptors. Cytokine Growth Factor Rev 16:139-149.

Ferrara N, Gerber HP, LeCouter J. 2003. The biology of VEGF and its receptors. Nat Med 9:669-676.

Herbst RS. 2004. Review of epidermal growth factor receptor biology. Int J Radiat Oncol Biol Phys 59:21-26.

Holmes G. 2012. Mouse models of Apert syndrome. Childs Nerv Syst 28:1505-1510.

Holmes G, Rothschild G, Roy UB, Deng CX, Mansukhani A, Basilico C. 2009. Early onset of craniosynostosis in an Apert mouse model reveals critical features of this pathology. Dev Biol 328:273-284.

Ibrahimi OA, Eliseenkova AV, Plotnikov AN, Yu K, Ornitz DM, Mohammadi M. 2001. Structural basis for fibroblast growth factor receptor 2 activation in Apert syndrome. Proc Natl Acad Sci U S A 98:7182-7187.

Jiang X, Iseki S, Maxson RE, Sucov HM, Morriss-Kay GM. 2002. Tissue origins and interactions in the mammalian skull vault. Dev Biol 241:106-116.

Kreiborg S, Cohen MM, Jr. 1990. Characteristics of the infant Apert skull and its subsequent development. J Craniofac Genet Dev Biol 10:399-410.

Lakso M, Pichel JG, Gorman JR, Sauer B, Okamoto Y, Lee E, Alt FW, Westphal H. 1996. Efficient in vivo manipulation of mouse genomic sequences at the zygote stage. Proc Natl Acad Sci U S A 93:5860-5865.

Oldridge M, Lunt PW, Zackai EH, McDonald-McGinn DM, Muenke M, Moloney DM, Twigg SR, Heath JK, Howard TD, Hoganson G, Gagnon DM, Jabs EW, Wilkie AO. 1997. Genotype-phenotype correlation for nucleotide substitutions in the IgII-IgIII linker of FGFR2. Hum Mol Genet 6:137-143.

Oldridge M, Zackai EH, McDonald-McGinn DM, Iseki S, Morriss-Kay GM, Twigg SR, Johnson D, Wall SA, Jiang W, Theda C, Jabs EW, Wilkie AO. 1999. De novo alu-element insertions in FGFR2 identify a distinct pathological basis for Apert syndrome. Am J Hum Genet 64:446-461.

Ornitz DM, Itoh N. 2001. Fibroblast growth factors. Genome Biol 2:REVIEWS3005.

Petiot A, Ferretti P, Copp AJ, Chan CT. 2002. Induction of chondrogenesis in neural crest cells by mutant fibroblast growth factor receptors. Dev Dyn 224:210-221.

Powers CJ, McLeskey SW, Wellstein A. 2000. Fibroblast growth factors, their receptors and signaling. Endocr Relat Cancer 7:165-197.

Shukla V, Coumoul X, Wang RH, Kim HS, Deng CX. 2007. RNA interference and inhibition of MEK-ERK signaling prevent abnormal skeletal phenotypes in a mouse model of craniosynostosis. Nat Genet 39:1145-1150.

Suzuki H, Suda N, Shiga M, Kobayashi Y, Nakamura M, Iseki S, Moriyama K. 2012. Apert syndrome mutant FGFR2 and its soluble form reciprocally alter osteogenesis of primary calvarial osteoblasts. J Cell Physiol 227:3267-3277.

Tanimoto Y, Yokozeki M, Hiura K, Matsumoto K, Nakanishi H, Matsumoto T, Marie PJ, Moriyama K. 2004. A soluble form of fibroblast growth factor receptor 2 (FGFR2) with S252W mutation acts as an efficient inhibitor for the enhanced osteoblastic differentiation caused by FGFR2 activation in Apert syndrome. J Biol Chem 279:45926-45934.

Wang Y, Sun M, Uhlhorn VL, Zhou X, Peter I, Martinez-Abadias N, Hill CA, Percival CJ, Richtsmeier JT, Huso DL, Jabs EW. 2010. Activation of p38 MAPK pathway in the skull abnormalities of Apert syndrome Fgfr2(+P253R) mice. BMC Dev Biol 10:22.

Wang Y, Xiao R, Yang F, Karim BO, Iacovelli AJ, Cai J, Lerner CP, Richtsmeier JT, Leszl JM, Hill CA, Yu K, Ornitz DM, Elisseeff J, Huso DL, Jabs EW. 2005. Abnormalities in cartilage and bone development in the Apert syndrome FGFR2(+/S252W) mouse. Development 132:3537-3548.

Wilkie AO, Slaney SF, Oldridge M, Poole MD, Ashworth GJ, Hockley AD, Hayward RD, David DJ, Pulleyn LJ, Rutland P, et al. 1995. Apert syndrome results from localized mutations of FGFR2 and is allelic with Crouzon syndrome. Nat Genet 9:165-172.

Yin L, Du X, Li C, Xu X, Chen Z, Su N, Zhao L, Qi H, Li F, Xue J, Yang J, Jin M, Deng C, Chen L. 2008. A Pro253Arg mutation in fibroblast growth factor receptor 2 (Fgfr2) causes skeleton malformation mimicking human Apert syndrome by affecting both chondrogenesis and osteogenesis. Bone 42:631-643.

Yu K, Herr AB, Waksman G, Ornitz DM. 2000. Loss of fibroblast growth factor receptor 2 ligand-binding specificity in Apert syndrome. Proc Natl Acad Sci U S A 97:14536-14541.

Figure legends

Fig. 1. Generation of the Apert mouse model with *sFGFR2IIIc*^{S252W}

(A) Genome structure of the region encompassing exons 6 and 7 of the FGFR2 gene in wild-type and mutant alleles. Primers a, b, and c and the length of PCR products are denoted. (B) Mating strategy and genotyping. Male mutant mice carrying *EIIa-Cre* and *sFGFR2IIIc*^{S252W} transgenes were first generated, and then crossed with *Fgfr2*$^{Neo\text{-}S252W}$ mice. Genomic DNA was extracted from tail tissue and subjected to PCR with the respective primer sets to determine the genotype. (C) Expression of soluble *FGFR2IIIc*^{S252W}. Serum was collected from *sFGFR2IIIc*^{S252W} mice and examined for soluble *FGFR2IIIc*^{S252W} by western blotting with an anti-FLAG antibody. The FLAG-BAP control fusion protein (Sigma) was used as a positive control.

Fig. 2. Gross appearance (A) and body weight (B) phenotypes

(A) Wild-type, *EIIa-Cre Fgfr2*$^{+/Neo\text{-}S252W}$ (Ap), and *EIIa-Cre sFGFR2IIIc*^{S252W} *Fgfr2*$^{+/Neo\text{-}S252W}$ (Ap/Sol) mice at P1. (B) Body weights of wild-type, Ap, and Ap/Sol mice. Mice (wild-type, Ap, and Ap/Sol) were weighed at P1. The thick lines indicate the median, and the upper and lower lines show the first and third quartile, respectively. $*p < 0.05$ (Dunn's test).

Fig. 3. Calvarial bone phenotypes

(A) Micro-CT images of the calvaria in wild-type (a, d, g), Ap (b, e, h), and Ap/Sol (c, f, i) mice at P1. Left (a–c), right (d–f), and frontal (g–i) views are shown. White arrowheads in b

and e and white arrows in g–i indicate premature fusion of the CS and the IFS, respectively. fb, frontal bone; pb, parietal bone. Scale bar, 2 mm. (B) Frontal views of the calvarial bone micro-CT analysis data of wild-type (a), Ap (b), and Ap/Sol (c) mice at P8 were used to reconstruct three-dimensional images with TRI/3-D-BON software. Red arrows in k indicate patency of the IFS. fb, frontal bone. Scale bar, 4 mm. (C) BMD of the parietal bone. BMD was calculated based on micro-CT data by TRI/3-D-BON software. The thick lines indicate the median, and the upper and lower lines indicate the first and third quartile BMD of the parietal bone, respectively. (D) IFS width at P1. IFS widths with a BMD threshold of 300 mg/cm^3 were measured based on the frontal micro-CT image. The thick lines indicate the median, and the upper and lower lines indicate the first and third quartile IFS widths, respectively.

Fig. 4. Histological analysis of the CS and IFS

(A) Sections of the CS were prepared from wild-type (a), Ap (b), and Ap/Sol (c) mice at P1. Sections were stained with H&E. The arrow in b indicates premature fusion of the CS in Ap mice. fb, frontal bone; pb, parietal bone. Scale bars, 50 μm. (B) Sections of the IFS were prepared from wild-type (a, d, g), Ap (b, e, h), and Ap/Sol (c, f, i) mice at P1. Sections were stained with H&E (a–c), Alizarin red (d–f), and Alcian blue (g–i). The arrowheads in b, e, and h indicate ectopic bones in the IFS of Ap mice. The yellow dashed lines in g, h, i indicate frontal bones. fb, frontal bone; pb, parietal bone. Scale bars, 100 μm.

Table 1 Genotyping of P1 pups.

	wild-type	*EIIa-Cre*	*sFGFR2IIIc*^{S252W}	*Fgfr2*$^{+/Neo\text{-}S252W}$	*EIIa-Cre* *Fgfr2*$^{+/Neo\text{-}S252W}$	*sFGFR2IIIc*^{S252W} *Fgfr2*$^{+/Neo\text{-}S252W}$	*EIIa-Cre* *sFGFR2IIIc*^{S252W}	*EIIa-Cre* *sFGFR2IIIc*^{S252W} *Fgfr2*$^{+/Neo\text{-}S252W}$
Mutant frequency (%)	13.22 (32/242)	23.14** (56/242)	17.77* (43/242)	8.26* (20/242)	10.74 (26/242)	15.70 (38/242)	7.03* (17/242)	4.13** (10/242)
Expected frequency (%)	12.5	12.5	12.5	12.5	12.5	12.5	12.5	12.5

* Statistically significant at $p < 0.05$

** Statistically significant at $p < 0.001$

Table 2 Incidence of AS-like phenotypes.

Phenotypes	Frequency			*p*-value		
	wild-type	Ap	Ap/Sol	wild-type vs Ap	Ap vs Ap/Sol	wild-type vs Ap/Sol
CS irregularity	0 % (0/16)	68.75 % (11/16)	0 % (0/12)	<0.0001***	0.0003***	1.0000
Widened IFS	0 % (0/9)	77.78 % (7/9)	50 % (3/6)	0.0023**	0.3287	0.0440
IFS with ectopic bones	0 % (0/9)	77.78 % (7/9)	0 % (0/6)	0.0023**	0.0070*	1.0000

* Statistically significant at $p < 0.05$ after Bonferroni correction.

** Statistically significant at $p < 0.01$ after Bonferroni correction.

*** Statistically significant at $p < 0.001$ after Bonferroni correction.

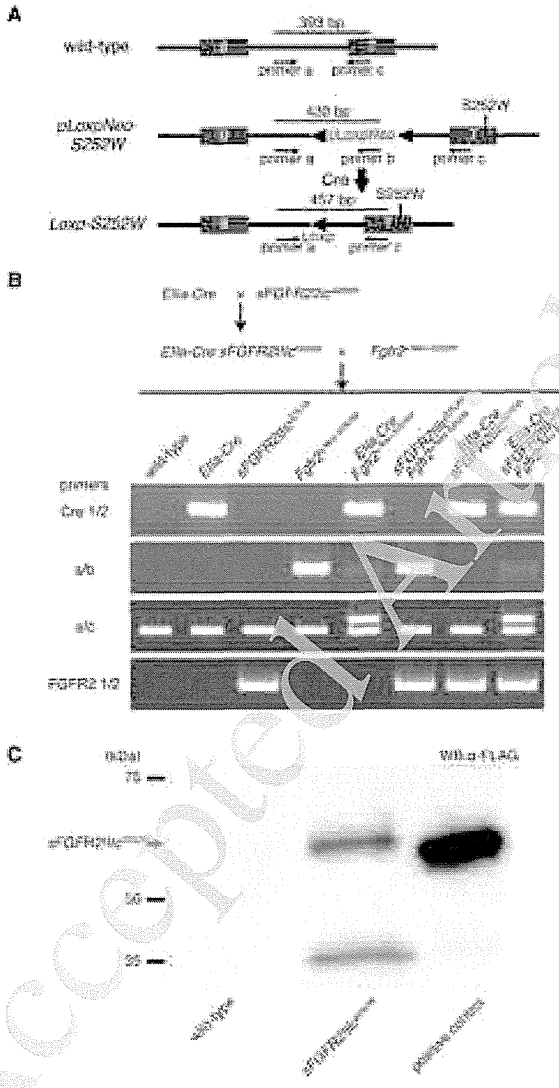

114x212mm (300 x 300 DPI)

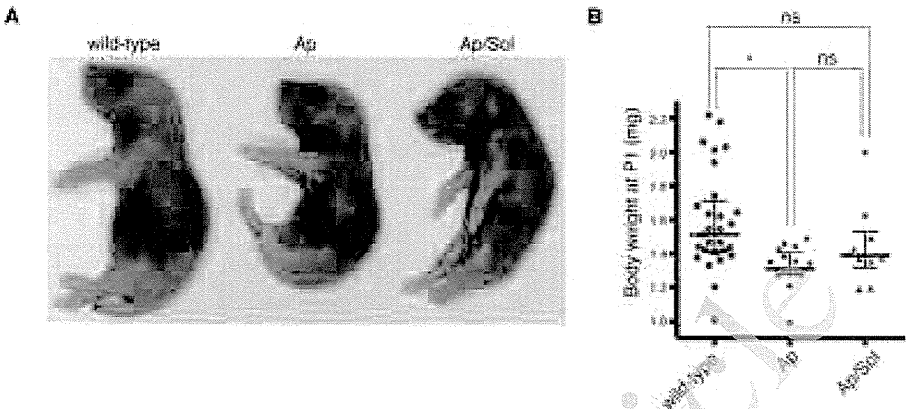

173x79mm (300 x 300 DPI)

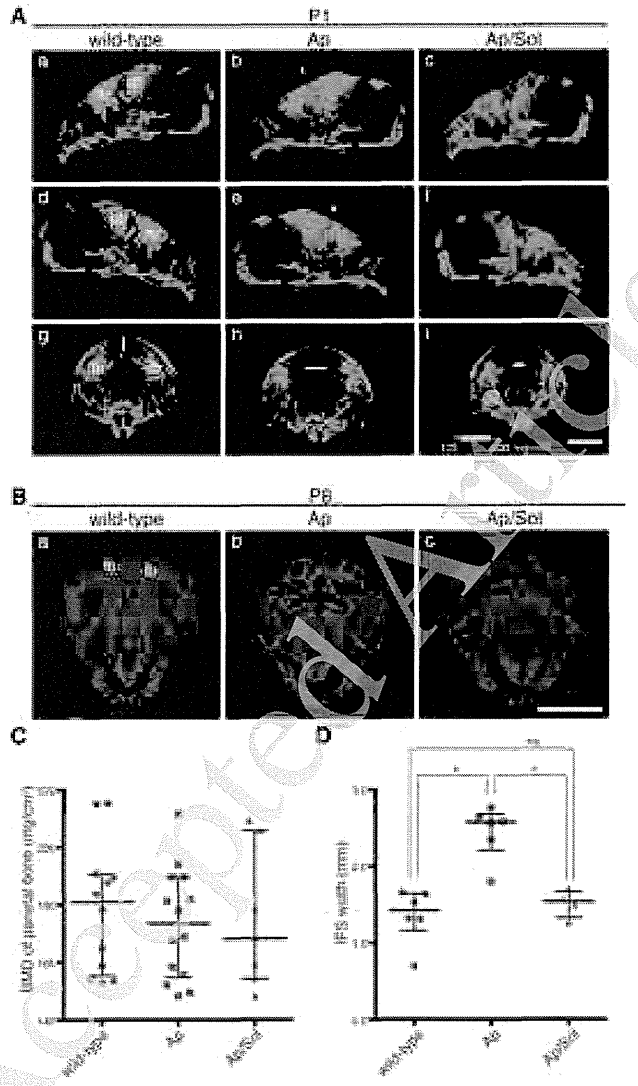

114x200mm (300 x 300 DPI)

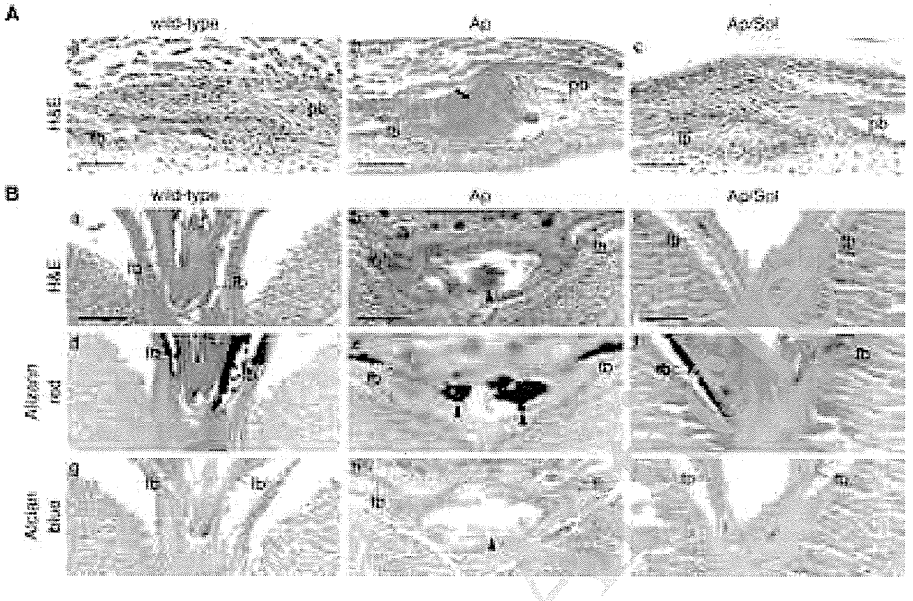

175x111mm (300 x 300 DPI)

CASE REPORT AJO-DO

Long-term stability of LeFort III distraction osteogenesis with a rigid external distraction device in a patient with Crouzon syndrome

Shingo Kuroda,[a] Keiichiro Watanabe,[b] Kyoko Ishimoto,[b] Hideki Nakanishi,[c] Keiji Moriyama,[d] and Eiji Tanaka[e]
Tokushima and Tokyo, Japan

A 6-year-old boy, diagnosed with Crouzon syndrome, had moderate exorbitism, a concave profile, an anterior crossbite of −4.0 mm, and a skeletal Class III jaw-base relationship caused by midfacial hypoplasia. At age 8 years 9 months, a LeFort III osteotomy was performed, and distraction osteogenesis was immediately started with the rigid external distractor system. The midface was advanced approximately 10.0 mm for 6 days, including overcorrection. After the distraction, a reverse headgear was used for 6 years to prevent relapse and to accelerate expected growth. At age 16 years 5 months, after extraction of the maxillary first premolars and mandibular third molars, 0.022-in preadjusted edgewise brackets were placed to treat the edge-to-edge incisor relationship and minor crowding. After 13 months of treatment, the facial profile was significantly improved, and an acceptable occlusion was achieved. During the 9-year observation period after the distraction, acceptable facial growth occurred, and no relapse of the maxillary advancement was observed. However, syndrome-specific growth and methodologically induced relapse should be considered when planning a LeFort III distraction in children for the treatment of Crouzon syndrome. (Am J Orthod Dentofacial Orthop 2011;140:550-61)

Crouzon syndrome is an autosomal dominant condition characterized by craniosynostosis with associated dentofacial anomalies.[1,2] Especially, exorbitism and midfacial hypoplasia are known as pathognomonic symptoms. Patients with Crouzon syndrome often require orthodontic or orthopedic treatment, because of their esthetic and functional problems, such as a Class III malocclusion and midfacial hypoplasia. For several decades, severe cases of Crouzon syndrome were treated mainly by maxillofacial advancement with LeFort III osteotomy, and this surgical procedure provides good treatment results with long-term stability.[3-9]

Recently, distraction osteogenesis has evolved as a new mainstream surgical technique for patients with jaw deformities since the first application of mandibular lengthening was reported in 1992.[10] Distraction osteogenesis for maxillary advancement started in 1993 and is now widely used in patients with skeletal Class III malocclusion caused by maxillary hypoplasia.[11-16] Two types of distraction devices have been used for maxillary advancement: internal and external. The rigid external distraction system, first reported in 1997 by Polley and Figueroa,[12] consists of the external distraction devices that have been used for a decade. This approach allows management of patients from childhood to adulthood, with excellent and predictable functional and esthetic outcomes.[12-16]

For the treatment of craniosynostosis, distraction osteogenesis is currently popular; several reports show the acceptable consequences of midfacial advancement.[17-22] A 1-year follow-up cephalometric study showed adequate stability of midfacial advancement with distraction osteogenesis in craniofacial dysostosis.[21] Fearon[22] also reported that the maxilla remained stable after LeFort III halo distraction without relapse

[a]Associate professor, Department of Orthodontics and Dentofacial Orthopedics, University of Tokushima Graduate School of Oral Sciences, Tokushima, Japan.
[b]Postgraduate student, Department of Orthodontics and Dentofacial Orthopedics, University of Tokushima Graduate School of Oral Sciences, Tokushima, Japan.
[c]Professor and chair, Department of Plastic and Reconstructive Surgery, Institute of Health Biosciences, University of Tokushima Graduate School, Tokushima, Japan.
[d]Professor and chair, Department of Maxillofacial Orthognathics, Tokyo Medical and Dental University Graduate School, Tokyo, Japan.
[e]Professor and chair, Department of Orthodontics and Dentofacial Orthopedics, University of Tokushima Graduate School of Oral Sciences, Tokushima, Japan.
The authors report no commercial, proprietary, or financial interest in the products or companies described in this article.
Reprint requests to: Shingo Kuroda, Department of Orthodontics and Dentofacial Orthopedics, University of Tokushima Graduate School of Oral Sciences, 3-18-15 Kuramoto-Cho, Tokushima 770-8504, Japan; e-mail, kuroda@dent.tokushima-u.ac.jp.
Submitted, November 2009; revised and accepted, December 2009.
0889-5406/$36.00

doi:10.1016/j.ajodo.2009.12.038

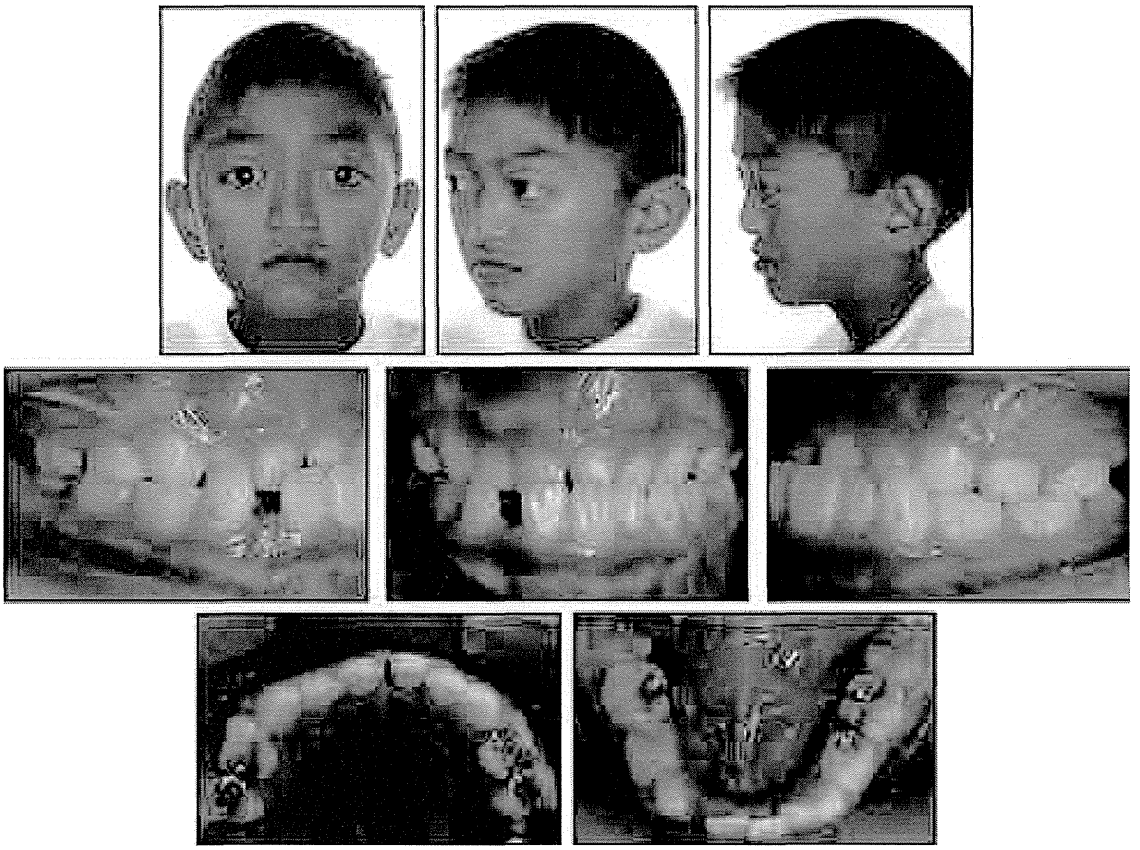

Fig 1. Pretreatment photographs.

for up to 5 years postoperatively. However, there are few reports of long-term detailed observation after LeFort III distraction in patients with Crouzon syndrome, and the prognosis of LeFort III distraction performed in childhood is still unclear.

This article demonstrates good prognosis for LeFort III distraction with the rigid external distractor system performed in the mixed dentition in a patient with Crouzon syndrome.

DIAGNOSIS AND ETIOLOGY

A boy, aged 6 years 8 months, had a chief complaint of anterior crossbite. He was diagnosed with Crouzon syndrome at Tokushima University Hospital in Japan, and his mother also has the same syndrome. He was suspected of having obstructive sleep apnea syndrome, since he had chronic nasal obstruction and significant snoring during sleep. Moderate exorbitism and a concave profile from midfacial hypoplasia were noted (Fig 1). An anterior crossbite of −4.0 mm was observed, and the terminal plane occlusion was a mesial-step type on both sides (Fig 2).

The cephalometric analysis, when compared with the Japanese norm, showed a skeletal Class III jaw-base relationship (ANB, −4.2°) because of a severe maxillary deficiency (SNA, 71.8°).[23] The body length and the ramus height of the mandible were almost in the normal range, but the facial convexity was significantly increased (Fig 3, Table).

TREATMENT OBJECTIVES

The patient was diagnosed as having a Class III malocclusion, with a skeletal Class III jaw-base relationship caused by midfacial hypoplasia. The treatment objectives were to (1) correct the midfacial hypoplasia and the concave facial appearance, (2) correct the anterior crossbite and establish ideal overjet and overbite, (3) achieve an acceptable occlusion with a good functional Class I occlusion, and (4) improve the tendency for sleep apnea with chronic nasal obstruction and significant

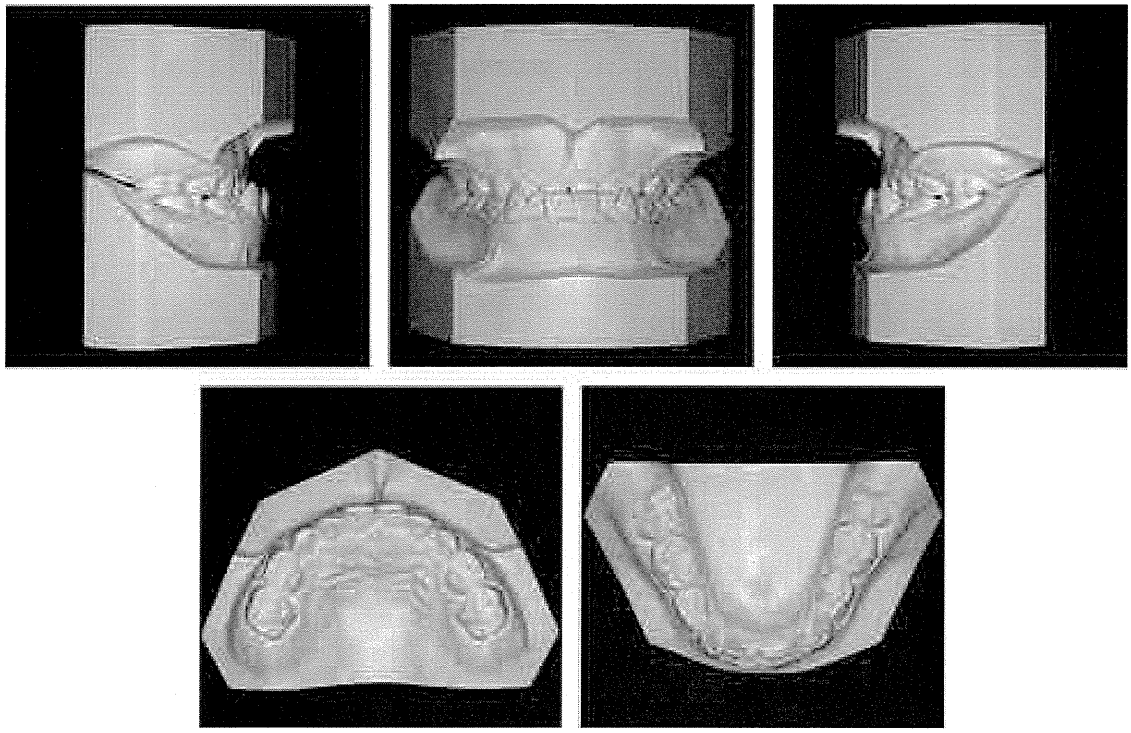

Fig 2. Pretreatment dental models.

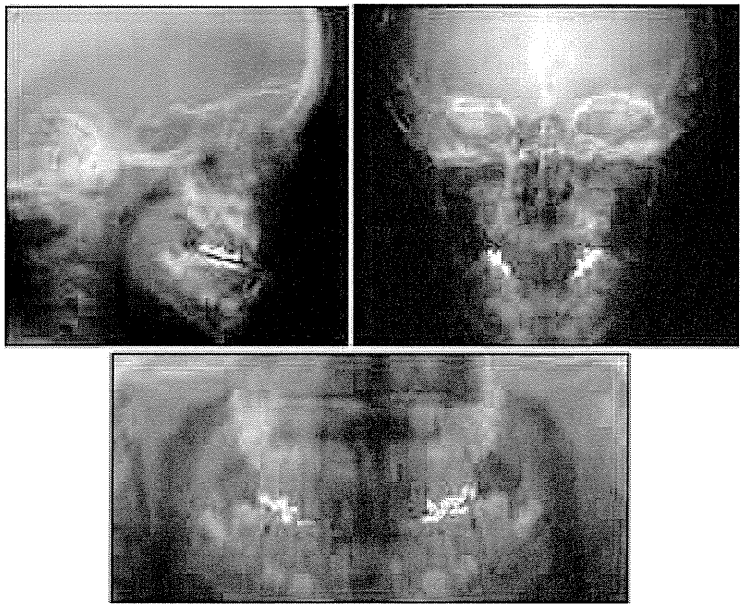

Fig 3. Pretreatment radiographs.

Table. Cephalometric summary

	Mean, Japanese male*				Pretreatment	Before DO	After DO			
							1 week	3 years	6 years	9 years†
Variables	8 y	SD	Adult	SD	6 y 9 mo	8 y 3 mo	8 y 9 mo	11 y 5 mo	14 y 5 mo	17 y 6 mo
Angle (°)										
ANB	4.9	1.9	3.2	2.4	−4.2	−4.0	3.1	2.9	2.7	3.1
SNA	81.8	3.7	81.5	3.3	71.8	71.9	76.5	77.1	76.8	76.8
SNB	76.9	3.4	78.2	4.0	76.0	75.9	73.4	74.2	74.1	73.7
MP-SN	37.6	4.2	34.5	6.1	33.4	31.8	32.9	31.5	34.9	37.0
Gonial angle	126.9	5.2	120.9	6.5	129.7	129.4	129.2	129.8	127.4	123.5
U1-SN	100.8	5.0	106.0	7.5	99.4	104.5	111.3	105.5	107.2	108.5
L1-MP	91.9	7.3	95.2	6.2	85.5	76.0	85.9	88.6	92.0	86.2
Convexity	168.3	4.2	173.2	5.5	200.3	203.7	184.0	182.0	185.7	182.7
Interincisal angle	129.4	9.7	124.2	8.6	141.7	147.7	130.0	134.5	125.9	128.3
Occlusal plane	20.5	3.0	15.5	4.2	11.7	12.9	12.4	11.6	10.2	12.1
Linear (mm)										
Point A to VRP	–		–		45.5	46.8	55.8	59.0	59.3	57.6
Pog to VRP	–		–		44.0	45.3	42.3	44.6	45.7	42.5
S-N	65.2	2.5	72.2	3.3	65.1	68.8	70.8	73.5	75.6	75.7
N-Me	111.4	4.0	135.7	4.0	107.1	112.3	114.4	119.6	129.8	140.9
N/palatal plane	48.9	1.8	60.0	1.8	43.3	45.9	48.9	50.0	53.5	60.4
Me/palatal plane	60.2	3.1	74.6	3.0	63.8	66.4	65.5	69.6	76.3	80.5
Ar-Go	40.4	2.2	53.2	5.7	43.3	45.1	44.7	46.5	48.6	53.3
Ar-Me	93.0	2.9	115.6	6.8	93.4	97.3	98.3	102.7	107.9	111.6
Go-Me	61.6	2.7	76.6	4.4	58.3	60.5	62.3	65.5	69.6	70.5
Overjet	2.8	1.4	3.3	1.0	−4.0	−3.5	5.9	3.0	0.5	2.1
Overbite	3.2	2.5	3.3	1.7	2.5	5.7	2.5	3.0	0.5	1.7

DO, Distraction osteogenesis; *VRP*, vertical reference plane (line perpendicular to SN line through S).
*Wada et al[23]; †End of active treatment.

snoring. Since the cause of the anterior crossbite, the prognathic profile, and the tendency of sleep apnea was suggested to have been the midfacial deficiency, we planned to advance the midface with distraction osteogenesis and LeFort III osteotomy after complete eruption of the maxillary incisors and first molars.

TREATMENT ALTERNATIVES

Several procedures were explored to achieve a proper facial profile and an acceptable occlusion. Although conservative treatment of maxillary growth modification with maxillary protraction headgear and then multibracket appliances were considered effective to improve the patient Class III malocclusion without surgical invasion, this method could not correct the severe skeletal disharmony caused by midfacial dysplasia, exorbitism, and sleep apnea.

So we planned surgical-orthodontic treatment to improve facial appearance. For midfacial advancement, we could use either a traditional LeFort III osteotomy and immediate repositioning of the distal fragment, or distraction osteogenesis after the osteotomy. Both procedures usually provide stable treatment results, but we chose distraction for this patient, since he was still growing and required a large amount of midfacial advancement to treat the midfacial dysplasia and exorbitism. We could also possibly plan the orthognathic surgery during adulthood, but continued impaired breathing could lead to obstructive sleep apnea.

For the distraction device, we selected a rigid external distractor system, because it has several advantages compared with the internal device: simple placement, flexibility to control the protraction direction, and no required second operation to remove the device.

TREATMENT PROGRESS

At the age of 7 years 5 months, the patient underwent a cranioplasty. At age 8 years 9 months, the LeFort III osteotomy was performed, and a rigid external distractor (KLS Martin, Tuttlingen, Germany) was placed on the cranial bones at the same time (Fig 4). Osteogenesis was started immediately after surgery. The maxilla was advanced approximately 10.0 mm over a 6-day period, including overcorrection. After distraction, the external device was kept in place for 4 weeks for rigid retention. Then a reverse headgear was used for 6 years for retention and to maximize any expected maxillary growth. All surgical procedures were performed in the

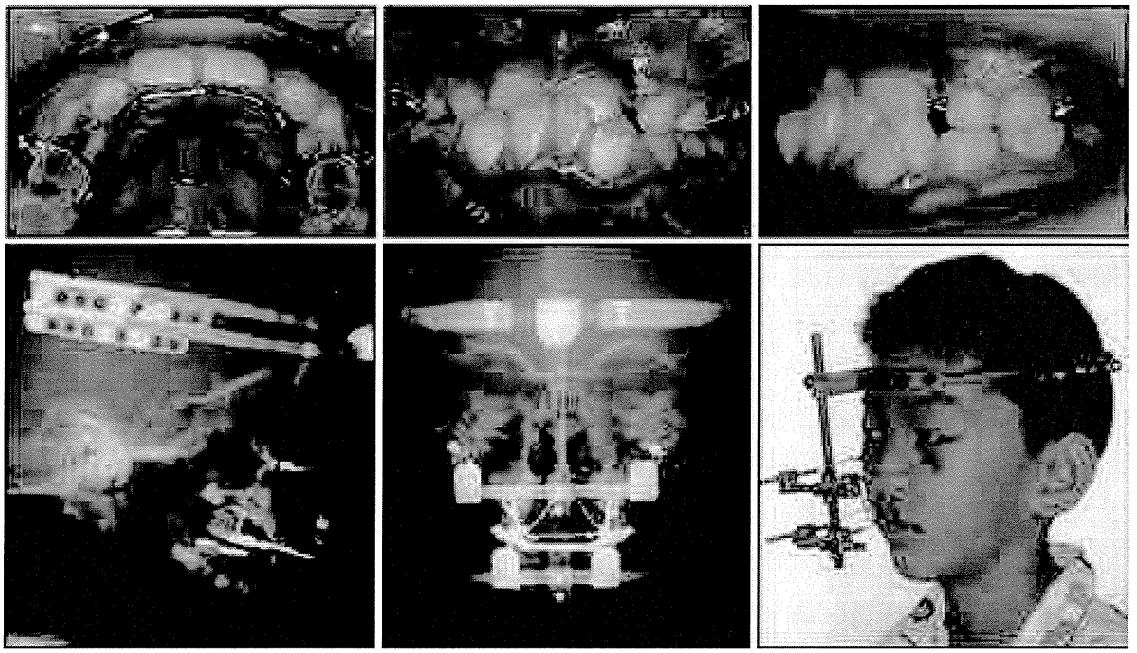

Fig 4. Photographs during the distraction osteogenesis.

Department of Plastic and Reconstructive Surgery at Tokushima University Hospital.

At age 10 years 7 months, the maxillary first premolars were extracted to allow eruption of the canines. At 15 years 5 months of age, a quad-helix appliance was placed for maxillary lateral expansion. At 16 years 5 months of age, after extraction of the mandibular third molars, 0.022-in preadjusted edgewise brackets were placed on both arches to improve the edge-to-edge incisor relationship and minor crowding. Short Class III and anterior box intermaxillary elastics were used for uprighting of the mandibular teeth and improvement of the interincisal relationships. The orthodontic treatment lasted for 13 months, and a circumferential retainer and bonded lingual retainers were placed in both arches for retention.

TREATMENT RESULTS

After distraction osteogenesis, the midfacial hypoplasia and exorbitism were dramatically improved, and the nasal obstruction had disappeared (Fig 5). Cephalometric evaluation at 1 week after distraction showed maxillary advancement of 9.0 mm at Point A relative to the SN plane and its perpendicular, and facial convexity was significantly improved (Figs 6 and 7). The posterior nasal spine was moved downward, and the mandibular plane angle was increased by 1.1°. The maxillary incisors were labially inclined, and the negative overjet was overcorrected to 5.9 mm. The deep overbite was reduced from 5.7 to 2.5 mm (Table).

Cephalometric evaluation 3 years after distraction showed a skeletal Class I jaw-base relationship (ANB, 2.9°). Significant anteroposterior growth of the anterior cranial base (S-N, 73.5 mm) and the maxillofacial complex (Point A to the vertical reference plane, 59.0 mm) was observed. An ideal interincisal relationship (overjet and overbite, 3.0 mm) was achieved by lingual inclination of the maxillary incisors (Figs 8, *A*, and 9).

Six years after distraction, a skeletal Class I jaw-base relationship (ANB, 2.7°) still remained; however, the mandibular plane angle had increased by 3.4°, and both overjet and overbite were reduced to 0.5 mm (Figs 8, *B*, and 9). The anterior cranial base (S-N) was increased to 75.6 mm.

Nine years after distraction, an acceptable facial profile was maintained (Fig 10). As the result of the multi-bracketed treatment, an ideal occlusion with Class II molar relationships and normal overjet and overbite were achieved (Fig 11). Posttreatment cephalometric evaluation showed the skeletal Class I jaw-base relationship (ANB, 3.1°) (Fig 12).

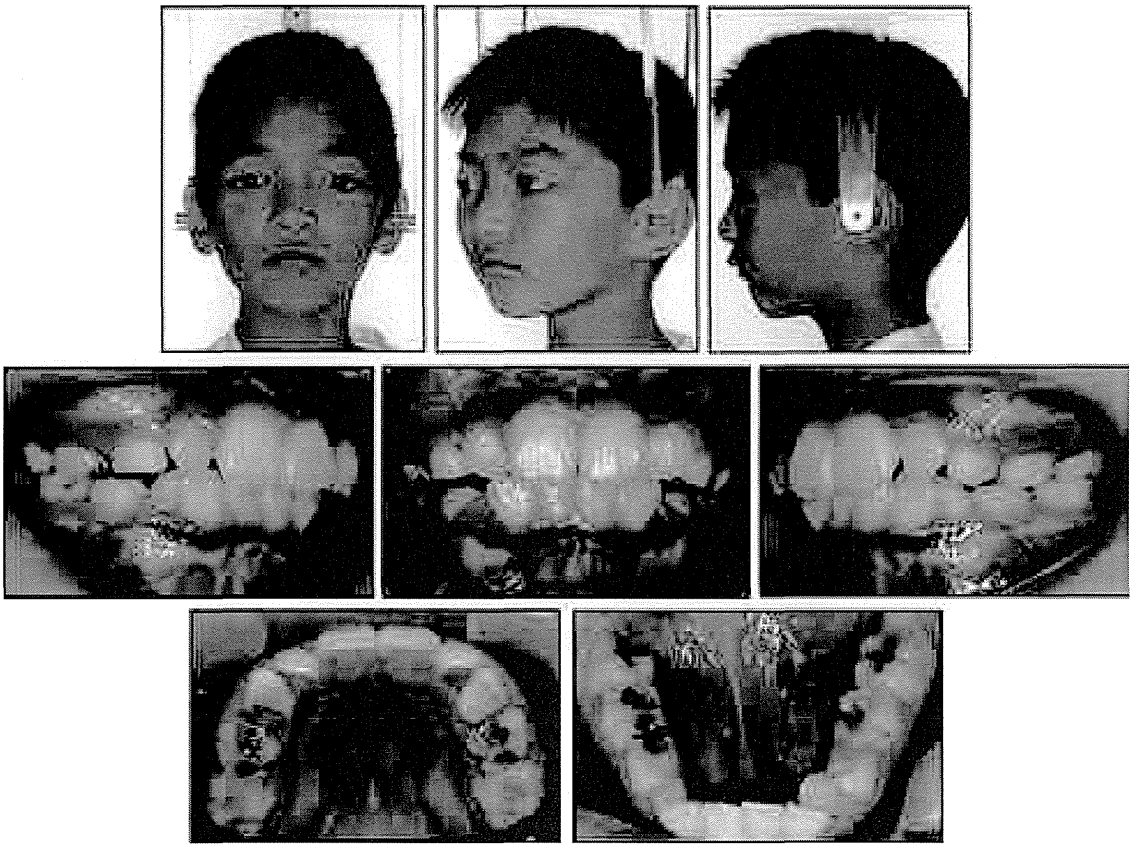

Fig 5. Photographs at 1 week after the distraction osteogenesis.

The increase of the mandibular ramus height and the decrease of the gonial angle were in the normal range through the whole observation period of 11 years; however, growth of the mandibular body length was significantly less than Japanese norms (Table).

DISCUSSION

In patients with Crouzon syndrome, midfacial hypoplasia causes several clinical problems, most notably at the level of the airway, orbits, occlusion, and facial esthetics. Nout et al[24] suggested that midface advancement can be scheduled in the first years of life for specific indications, such as severe obstructive sleep apnea or severe exorbitism. Our patient had nasal obstruction and significant snoring at the initial examination, and sleep apnea was suspected. In addition, he showed a skeletal Class III jaw-base relationship with an anterior crossbite, a concave profile, and moderate exorbitism. Therefore, early surgical treatment was proposed to improve both functional and morphologic problems with their associated psychosocial issues. During early treatment of midfacial hypoplasia with orthognathic surgery, several reports indicated that distraction was more suitable than conventional osteotomy.[24-28] Distraction osteogenesis can overcome the natural soft-tissue resistance by gradual stretching and accommodation, generating new soft tissues simultaneously with skeletal augmentation. Active craniofacial growth in childhood can facilitate both new bone generation and its succeeding soft-tissue adaptation. Furthermore, distraction provides less physical and psychological invasion: ie, reduced operating time, less blood loss, less postoperative pain, and shorter hospitalization.[24,25] Therefore, we selected the distraction option combined with the LeFort III osteotomy for this patient.

As a result of the 9-mm maxillary distraction, facial esthetics were improved significantly, and the negative overjet was overcorrected. In the comparison of the

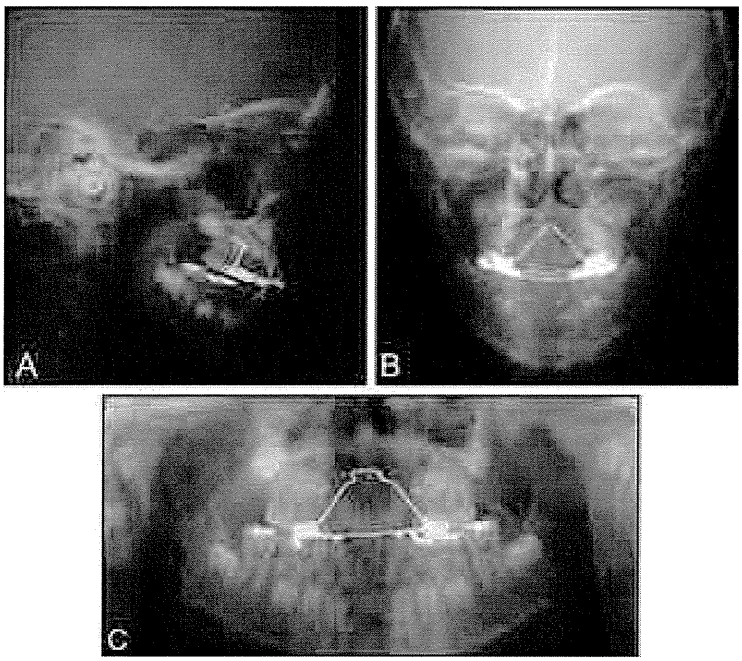

Fig 6. Radiographs at 1 week after the distraction osteogenesis: **A,** lateral cephalograph; **B,** frontal cephalograph; **C,** panoramic radiograph.

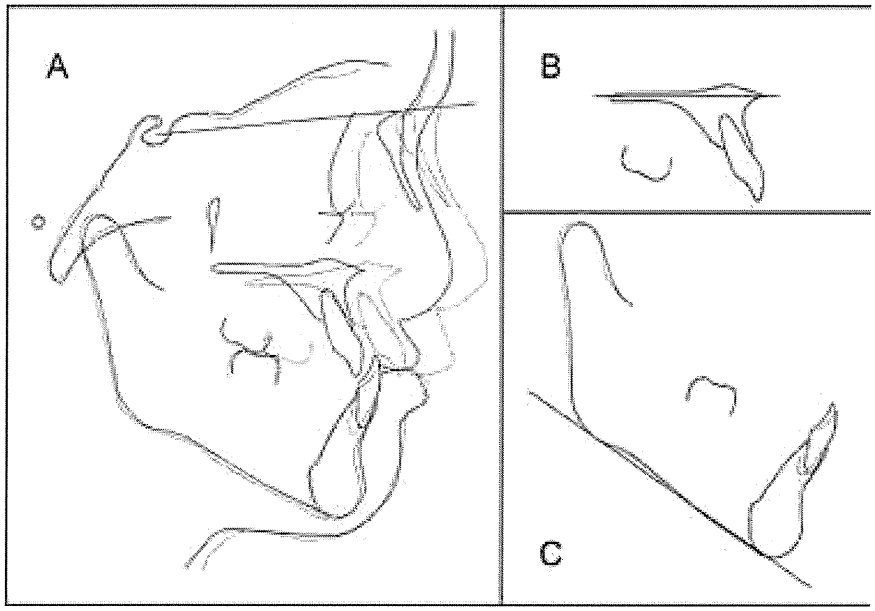

Fig 7. Predistraction (solid line) and 1 week after the distraction osteogenesis (dotted line) cephalometric tracings: **A,** superimposed on sella-nasion plane at sella; **B,** superimposed on the palatal plane at ANS; **C,** superimposed on the mandibular plane at menton.